Current progress in the magnetism of rare-earth–hydrogen systems

P. Vajda*

Laboratoire des Solides Irradiés, Ecole Polytechnique, F-91128 Palaiseau, France

Abstract

We are reviewing recent progress obtained in the study of hydrogen interaction with magnetic structures in rare-earth metals, emphasizing the role of the ordering state of the H-sublattice. We shall present in particular: (1) the situation in the solid solutions of the heavy rare earths, α^*-RH$_x$, and the efforts to relate the special quasi-unidimensional configuration of this phase (charge-density waves) to their modulated magnetism (spin-density waves) via the Fermi surface; (2) an assembly of all magnetic structures determined up to now in the heavy-RE dihydrides, β-RH(D)$_{2(+x)}$, for a tentative comparison of the observed commensurate and/or incommensurate configurations; special mention will be made of the remarkably stable short-range ordered (SRO) magnetism always present in these systems; (3) the need for further (thorough) neutron scattering work on the magnetism in the insulating R-trihydrides, γ-RH(D)$_{3(-x)}$, in order to specify its mechanism in the absence of RKKY exchange interaction.
© 2005 Elsevier B.V. All rights reserved.

Keywords: Rare earths; Magnetism; Solid solutions; Hydrides; Order–disorder

1. Introduction

The rare-earth–hydrogen (R–H) phase diagram as presented in Fig. 1 is generally valid for the hcp lanthanides Gd through Lu (with some reservations for Yb: there, only above 2.3 atoms H/R) and for the assimilated Sc and Y. It is characterized by relatively broad existence ranges around the stoichiometric compositions, both in the α-phase solid solutions and for the cubic β-phase di- and hcp γ-phase trihydrides. An extensive review of the situation has been given in Ref. [1].

As concerns the magnetic properties of the rare earths with incomplete 4f-shells, their interaction with hydrogen is favoured by the stability of the single-phase regions of Fig. 1 at low temperatures, where these metals are magnetically ordered. The particularly exciting case of the metastable low-T α^*-phase will be treated in more detail later. In Table 1, we show the (upper) phase limits for this group of metals in the α^*-phase and in the β-phase. (The values have been taken from Ref. [1] and from more recent refined neutron work by Udovic et al. [2].) The lower limits of the β-phase are purity dependent and reach ideally values close to 2.00; the width of

the γ-phase has not been established definitely in most cases but is of the order of 0.1 atoms H/R. We note already now the possibility of studying the magnetism in solid solutions of Ho, Er, and Tm and the possible existence of magnetic dihydrides from Gd to Tm. (Cubic TmH$_2$ is a van Vleck paramagnet with a non-magnetic ground state.) An additional important characteristic following from the phase diagram is the tendency of the excess hydrogens "x" in each phase to form sub-lattices at higher x and lower T, with a strong influence upon electronic and thus magnetic properties. In the following, we shall discuss the present situation for each part of the phase diagram and the corresponding wishes and outlooks.

2. Results and discussion

2.1. α^*-RH$_x$ solid solution phase

As mentioned above, the unusual fact of an existing H solid solution phase down to the lowest temperatures, without precipitation of the dihydride, has permitted to study its interaction with magnetism in Ho, Er, and Tm. Thus, it was found (for details and references, see Ref. [1]) that the transition temperatures to sinusoidal or helical antiferromagnetism

* Tel.: +33 1 69 33 45 09; fax: +33 1 69 33 30 22.
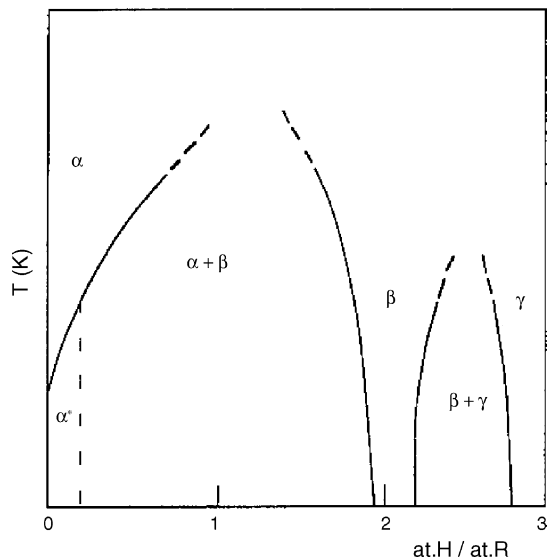 *E-mail address:* peter.vajda@polytechnique.fr.

Fig. 1. Typical R–H phase diagram for the hcp rare earths showing extended single-phase non-stoichiometric regions.
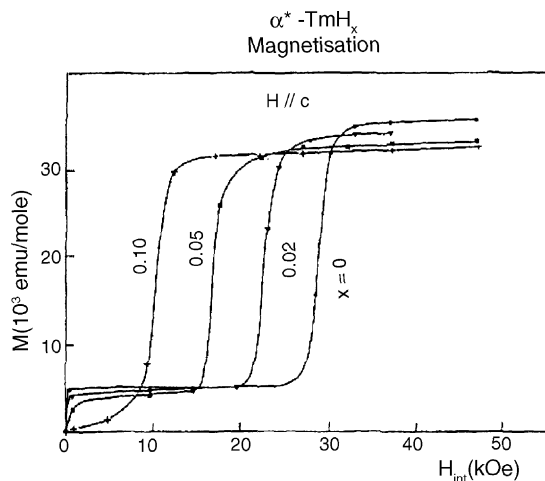

Fig. 2. Magnetization of α^*-TmH$_x$ as a function of applied field at 4.3 K showing easier spin-flip transformation with hydrogen (after [3]).

(AFM), T_N or T_H, decreased in all three metals as well as the T_C towards ferrimagnetism in Tm, while the T_C towards conical ferromagnetism (FM) in Er increased strongly upon hydrogenation. At the same time, a kind of magnetic hardening took place manifesting itself e.g. by a decrease of the critical field needed for the ferri-to-ferromagnetic spin-flip transition in Tm (Fig. 2) or by the increasing spiral period of the helical phase in Ho (Fig. 3). The observations were explained by the competition of several processes: on the one hand, a diminishing role of the RKKY exchange mechanism due to a decrease of the carrier density with increasing H concentration and, on the other, by a simultaneously growing influence of magneto-elastic and anisotropy effects.

It is useful to recall, in this context, the special configuration of the α^*-phase which, in fact, is not a real solid solution but – as determined by neutron scattering (see [1] for details) – consists of H–R–H pairs on second-neighbour T-sites aligned in modulated quasi-unidimensional chains along the c-axis. And this reminds one at once of the equally modulated AFM of the here discussed rare earths, where the α^*-phase is present. Fig. 4 shows this parallelism between the spin-density waves (SDW) in the concerned metals and the charge-density wave (CDW) formed by the zig-zagging structure of the α^*-phase. As noted earlier [5], not only the alignment but

also the modulation period i.e. the turning angle, ω_i, between successive basal planes—is roughly the same: $(7$–$7.5)c/2$ or $\omega_i = 48$–$51°$, in all cases. This has induced us to relate the occurrence of the CDW of the α^*-phase to an electronic topological transition on the Fermi surface, in particular to its webbing features. It was shown that the α^*-phase was only observed in systems where the nesting vector **q** connecting the webbing regions of the Fermi surface and directly related to the interlayer turning angle, $|\mathbf{q}| = \omega_i 2/c$, corresponded to a $\omega_i \approx 50°$. Such a situation turned out to be close to a Peierls transition and was propitious for modulated unidimensional

Table 1
Phase boundaries in the α^* (Part a) and in the β-phase (Part b)

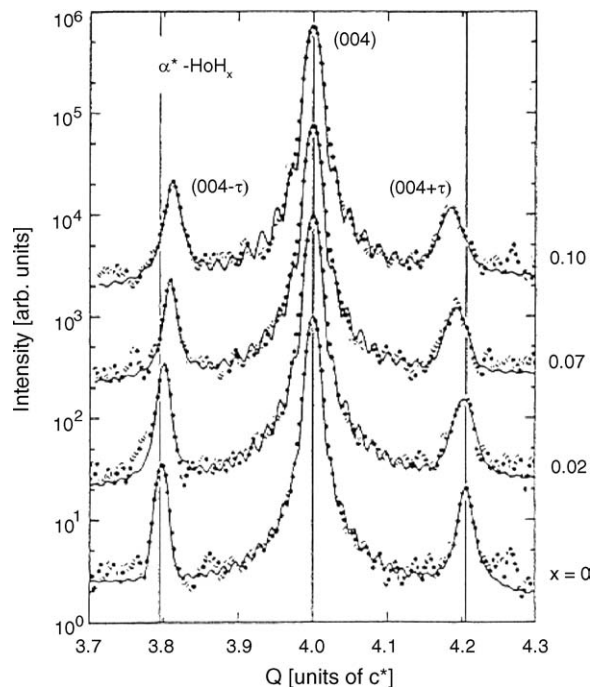| (a) $x(\alpha^*)_{max}$		(b) $(2+)x(\beta)_{max}$	
Sc	0.35	Gd	0.30
Y	0.21	Tb	0.25
Ho	0.03	Dy	∼ 0.20
Er	0.06	Ho	0.15
Tm	0.11	Er	0.09
Lu	0.20	Tm	0.06
		Lu	0.03

Fig. 3. Magnetic X-ray scattering across the (0 0 4) Bragg peak in α^*-HoH$_x$ at 40 K showing decreasing satellite separation, i.e. increasing spiral period of the helical phase (after [4]).
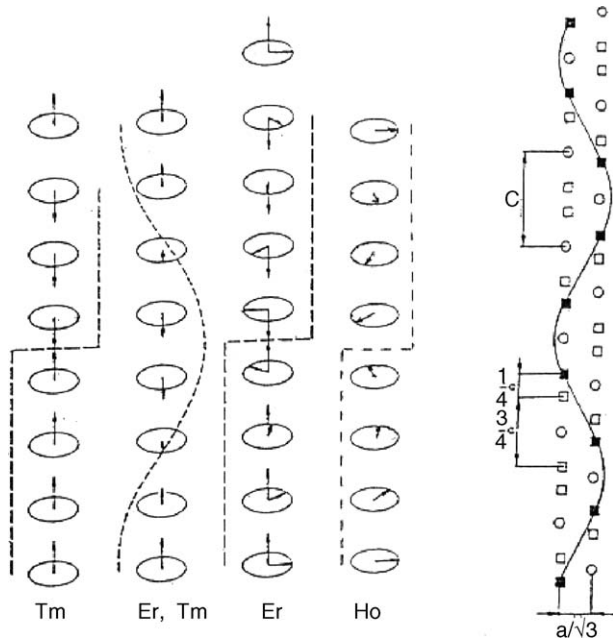
Fig. 4. *c*-Axis modulated magnetic configurations (SDW) in Ho, Er, and Tm (to the left) and the modulated H–R–H chain structure (CDW) of the α*-phase (to the right).
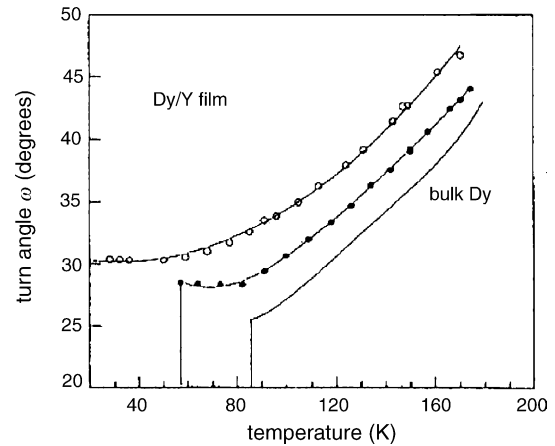

Fig. 5. *T*-dependence of the interlayer turning angle ω_i in the helical phase of Dy/Y epitaxial films for two Dy thicknesses: 3200 Å (filled circles) and 600 Å (open circles) (after [8]).

manifestations such as CDW and SDW. The three metals with modulated configurations exhibiting a ω_i closest to this value are just those possessing an α*-phase, while the equally modulated AFM of Dy and Tb with much smaller ω_i, ~40° and 20° respectively near T_N, explains why they are not apt for it; this is even more so for the permanently FM Gd with $\omega_i = 0$. We have tested [6] these ideas on the alloy system $Y_y Tb_{1-y} H(D)_x$ and confirmed the existence of the α*-phase in the case of $y = 0.9$ with $\omega_i = 50°$ for its AFM modulation but not for that of $y = 0.2$ with its $\omega_i = 32°$ only. Theoretical efforts to study the eventual evolution of the Fermi surface upon introduction of hydrogen have been undertaken (to begin with) on the non-magnetic YH_x system [7].

It is also interesting to note that the above described phenomenon is quite general and observed in systems outside the M–H field. Thus, clamping effects on Dy/Y epitaxial films leading to orthorhombic distortion increase the turning angle ω_i via magneto-elastic interaction and favour the SDW of the helical phase [8]. We note (Fig. 5) that the initially too low ω_i of ~40° near T_N of bulk Dy increases up to 48° for a 600 Å thick Dy/Y film suggesting that the latter might already exhibit an observable α*-phase when loaded with H. Similarly,

strong electron–phonon coupling in deposited layers of halogen bridged chains on platinum, Pt–Br–Pt, yields nesting on the Fermi surface with lattice distortion and the associated CDW [9]. Finally, zig-zagging CDW are induced in hexagonal Nb_3Se_4 by intercalating In atoms which – through lattice distortion – drive the system close to a Peierls transition [10].

2.2. β-Phase dihydrides

2.2.1. Pure β-RH₂ systems

The situation for the systems with R = Tb, Dy, and Ho has been relatively well established by neutron scattering (Refs. [1,11,12]) and is summarized in Table 2. We note, at low *T*, a general presence of two overlapping sinusoidally modulated AFM configurations: that at higher *T* with an incommensurate propagation vector $\mathbf{k}_2$ being replaced at lower *T* by a more commensurate one. (GdD₂ is also AFM below 18 K, but possessing a MnO-type structure with a $\mathbf{k} = 1/2[1\,1\,1]$, similar to that of SmD₂ and indicating that it should rather belong to the light RE group.) We have added recent yet unpublished results on ErD₂ obtained together at Saclay and at NIST [13] and which confirm the great similarity of the incommensurate configurations at higher *T*'s. A difficulty is the fact that – contrarily to the expectations – no second (commensurate?) AFM configuration could be detected down to 120 mK. Whether it might show up at even lower *T* is an open question.

Table 2
Magnetic configurations and transition temperatures in pure RD₂ (R = Tb,Dy,Ho,Er)

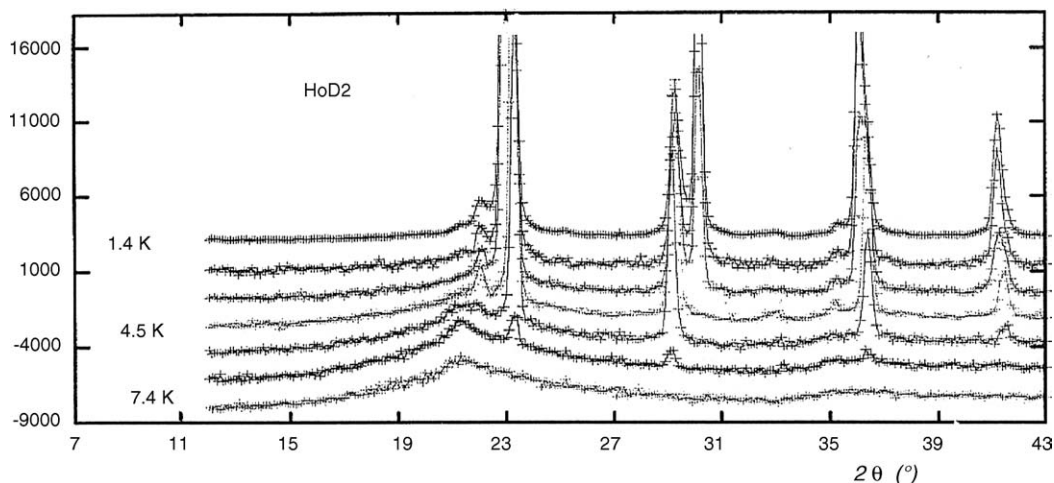|	$\mathbf{k}_1$	$\mathbf{k}_2$	T_1 (K)	T_N (K)
TbD₂	1/4(1 1 3)	≈ 1/8(116)	15–16	19
DyD₂	≈ 1/4(1 1 3)	1/40(11,11,30)	3–3.5	5.2
HoD₂	1/4(1 1 3)	1/40(11,11,30)	3–4	6.3
ErD₂	?	1/40(11,11,30) and ≈ 1/8(116)	?(<0.12)	2.3

Fig. 6. Neutron diffraction spectra for HoD$_2$ for various temperatures showing coexistence of magnetic SRO and LRO (after [12]).

Another interesting phenomenon is the appearance within the magnetically ordered range, in at least three RD$_2$ systems (with R = Tb, Ho, and now Er), of additional magnetic SRO lines persistent far above the respective T_N's—up to 3–4 times their value. An example is shown in Fig. 6 for HoD$_2$ from where one concludes on correlation lengths ξ_c between 20 and 50 Å decreasing with increasing T. It is also notable that the lines (two can be distinguished) are peaking at about the same positions in all three systems, at $2\Theta = 21°$ and $\sim35°$; we shall come back to this later.

2.2.2. Superstoichiometric β-RH $_{2+x}$ systems

It had already been noted earlier (e.g. in [1]) that the introduction of octahedral excess x-atoms affected the magnetic manifestations in various ways. First, at small x values, they act as structural and electronic perturbations resulting in a decreasing T_N and LRO—the peaks broaden. Second, when the concentration of x-hydrogens is high enough (and the temperature low enough) to interact, they form an ordered sublattice, which is usually of lower symmetry and can yield new LRO magnetism with sometimes an even higher T_N than for $x = 0$. (The resulting possibility of quenching across the sublattice ordering region around 150–200 K adds another parameter to "play with" as already shown e.g. with β-TbD$_{2+x}$ [14].)

It is encouraging that quite analogous phenomena have been recently studied on hydrides of R-intermetallics (and also reported at this conference). Thus, the interplay of magnetism with H superstructures was demonstrated through the appearance of SRO AFM lines in frustrated Laves hydrides Tb(Mn$_{1-y}$Al$_y$)$_2$H$_x$ as a function of x by Goncharenko et al. [15], while Figiel et al. [16] observed the appearance of non-collinear canted ferrimagnetism in hexagonal ErMn$_2$H$_x$ after an H-induced structural transformation at 220–250 K for $x = 3.5$–4.5.

Finally, let us come back to the persistent SRO magnetism mentioned above, and which has also been observed in some superstoichiometric systems such as β-HoD$_{2.12}$ [12]. There, the lines were strong enough to induce us to try a fit for closer analysis. Surprisingly, the magnetic SRO spectra in these purely *cubic* systems could only be fitted when using the *hexagonal* cell of the corresponding trihydrides. This reminds of a martensitic-type memory mechanism signalling an electronic phase separation such as proposed for magnetic oxides exhibiting colossal magnetoresistance and described e.g. in [17]. Though never invoked for metal hydrides it could also be the basic mechanism for the metal–insulator transitions observed in β-YH$_{2.1}$ and other superstoichiometric R-dihydrides near the phase boundary [1,18], with the presence of coherent (microscopic) insulating γ-phase regions within the metallic β-phase.

2.3. γ-Phase trihydrides

Very little new work has been done since the last review [1] for the characterization of magnetic trihydrides. The interaction is mostly dipole–dipole, with large crystal-field effects, but no RKKY exchange because of the absence of carriers in these insulating materials. A nice example was the Ce–H system [1], where the trihydride (though not really a γ-phase since cubic) exhibited the same AFM-coupled (1 1 1) planes as the dihydride but without its modulation.

More recently, Udovic et al. [19] had determined the magnetic structure of DyD$_3$ by neutron scattering as AFM-stacked FM planes along the c-axis of the type *aabb* confirming the earlier observed transition temperature of $T_N = 3.3$ K. And finally, let us mention for the sake of completeness, an NMR study by Weizenecker [20] showing that γ-TmH$_{2.73}$ remains a van Vleck paramagnet, just like the cubic β-TmH$_2$, but the splitting between the non-magnetic ground state, Γ_2, and the first excited magnetic state, $\Gamma_5^{(2)}$, has decreased by more than 1/3: from 174 to 111 K.

3. Conclusions

Summarizing the situation of magnetism in the three regions of the R–H phase diagram one can state the following:

- For the α^*-RH$_x$ (R = Ho, Er, Tm) solid solutions, the observations concerning the transition temperatures seem rather complete but qualitative information by magnetic XRD and ND would be interesting; investigation of its possible connection with the shape of the Fermi surface is desirable, both experimentally (photo-emission, angular resolved positron annihilation) and theoretically (band structures).
- In the case of pure β-RH(D)$_2$, the determination of the magnetic structures is nearly complete; for superstoichiometric β-RH(D)$_{2+x}$ (R = Tb, Dy, Ho), it is well advanced owing to neutron and also to muon spin relaxation (muSR) [21] spectroscopy. More magnetic scattering is required on ErH(D)$_{2+x}$ (in progress) and GdH(D)$_{2+x}$ (despite the "prohibitive" neutron properties of the Gd nucleus). The martensitic "memory" effects of the magnetic SRO are not understood yet, and band structure calculations including the 4f-magnetism as well as H-sublattice order phenomena should be tempted.
- Magnetic transitions have been determined for (Ce, Nd, Gd, Dy, Er) trihydrides; structures only for DyD$_3$ (and CeD$_3$). Magnetic scattering experiments are required for all other RH(D)$_3$ and all γ-RH(D)$_{3-x}$ systems. Band structure calculations including the 4f-magnetism as well as VacH-sublattice order phenomena (also in connection with eventual M–I transitions) should be tempted.

References

[1] P. Vajda, in: K.A. Gschneidner (Ed.), Handbook on the Physics and Chemistry of Rare Earths, vol. 20, North Holland, 1995.
[2] T.J. Udovic, Q. Huang, J.J. Rush, J. Alloys Compd. 356/357 (2003) 41.
[3] J.N. Daou, J.P. Burger, P. Vajda, G. Chouteau, R. Tur, J. Phys.: Condens. Matter 2 (1990) 7897.
[4] C. Sutter, D. Labergerie, A. Remhof, H. Zabel, C. Detlefs, Europhys. Lett. 53 (2001) 257.
[5] P. Vajda, Physica B 289/290 (2000) 435.
[6] P. Vajda, O.J. Zogal, Phys. Rev. B 59 (1999) 9467;
    Y. Nakamura, P. Vajda, O.J. Zogal, E. Akiba, J. Alloys Compd. 356/357 (2003) 105.
[7] J. Garces, J.L. Gervasoni, P. Vajda, J. Alloys Compd. 404–406 (2005) 126–130.
[8] K. Dumesnil, C. Dufour, Ph. Mangin, G. Marchal, M. Hennion, Europhys. Lett. 31 (1995) 43.
[9] K. Swamy, A. Menzel, R. Beer, E. Bertel, Phys. Rev. Lett. 86 (2001) 1299.
[10] G.A. Scholz, Sol. State Ionics 149 (2002) 131.
[11] P. Vajda, G. André, J. Hammann, Phys. Rev. B 55 (1997) 3028.
[12] P. Vajda, G. André, O.J. Zogal, Phys. Rev. B 57 (1998) 5830.
[13] P. Vajda, G. André, T.J. Udovic, R.W. Erwin, Q. Huang, Phys. Rev. B 71 (2005) 054419.
[14] P. Vajda, J.N. Daou, G. André, Phys. Rev. B 48 (1993) 6166.
[15] I.N. Goncharenko, P. Cadavez-Peres, I. Mirebeau, O.L. Makarova, T. LeBihan, M. Mazouar, Phys. Rev. B 68 (2003) 214418.
[16] H. Figiel, A. Budziak, P. Zachariasz, J. Zukrowski, G. Fischer, G. Dormann, J. Alloys Compd. 368 (2004) 260.
[17] B. Raveau, A. Maignan, Europhys. News 34 (2003) 238.
[18] P. Vajda, J.N. Daou, Phys. Rev. Lett. 66 (1991) 3176.
[19] T.J. Udovic, Q. Huang, J.W. Lynn, R.W. Erwin, J.J. Rush, Phys. Rev. B 59 (1999) 11852.
[20] J. Weizenecker, Ann. Phys. (Leipzig) 10 (2001) 561.
[21] F.N. Gygax, P. Vajda, D. Andreica, M. Pinkpank, A. Schenck, J. Alloys Comp. 330/332 (2002) 376.